Received: 9 February 2022 | Revised: 8 March 2022 | Accepted: 14 March 2022

DOI: 10.1002/oby.23435

Obesity A Research Journal | THE OBESITY SOCIETY | WILEY

ORIGINAL ARTICLE

Obesity Biology and Integrated Physiology

Obesity accelerates acute promyelocytic leukemia in mice and reduces sex differences in latency and penetrance

John W. R. Kincaid[1,2,3] | Gretchen Weiss[1] | Anne E. Hill-Baskin[1] | Heidi M. Schmidt[1] | Ovwoioise Omoijuanfo[1] | Cheryl L. Thompson[2,3] | Rose C. Beck[3,4] | Nathan A. Berger[1,3,5]

[1]Center for Science, Health & Society, Case Western Reserve University, Cleveland, Ohio, USA

[2]Department of Nutrition, Case Western Reserve University, Cleveland, Ohio, USA

[3]Case Comprehensive Cancer Center, Case Western Reserve University, Cleveland, Ohio, USA

[4]Department of Pathology, Case Western Reserve University, Cleveland, Ohio, USA

[5]Departments of Medicine, Biochemistry, Genetics, and Genome Sciences, Case Western Reserve University, Cleveland, Ohio, USA

Correspondence
Nathan A. Berger, Center for Science, Health & Society, Case Western Reserve University, 10900 Euclid Ave., Health Sciences Library, 1st Floor Office, Cleveland, OH 44106-4971, USA.
Email: nab@case.edu

Funding information
This research was supported in part by NIH grants NCI P30 CA043703 and NCI R25 CA225461. The funders had no role in the design or conduct of the study; in the collection, management, analysis, or interpretation of the data; in the preparation, review, or approval of the manuscript; or in the decision to submit the manuscript for publication.

Abstract

Objective: Obesity has emerged as a prominent risk factor for multiple serious disease states, including a variety of cancers, and is increasingly recognized as a primary contributor to preventable cancer risk. However, few studies of leukemia have been conducted in animal models of obesity. This study sought to characterize the impact of obesity, diet, and sex in a murine model of acute promyelocytic leukemia (APL).

Methods: Male and female C57BL/6J.mCG$^{+/PR}$ mice, genetically predisposed to sporadic APL development, and C57BL/6J (wild type) mice were placed on either a high-fat diet (HFD) or a low-fat diet (LFD) for up to 500 days.

Results: Relative to LFD-fed mice, HFD-fed animals displayed increased disease penetrance and shortened disease latency as indicated by accelerated disease onset. In addition, a diet-responsive sex difference in APL penetrance and incidence was identified, with LFD-fed male animals displaying increased penetrance and shortened latency relative to female counterparts. In contrast, both HFD-fed male and female mice displayed 100% disease penetrance and insignificant differences in disease latency, indicating that the sexual dimorphism was reduced through HFD feeding.

Conclusions: Obesity and obesogenic diet promote the development of APL *in vivo*, reducing sexual dimorphisms in disease latency and penetrance.

INTRODUCTION

Acute promyelocytic leukemia (APL), a subtype of acute myeloid leukemia, has recently been identified as an obesity-associated cancer (OAC) (1). Obesity has, in fact, been clearly linked to increased risk of multiple malignancies and worse outcomes for patients with these OACs (2). Murine models for solid tumors have been useful to better understand and disrupt the obesity–cancer linkage (3-10); however, no animal model of APL has been evaluated for the effect of obesity on disease development, penetrance, or latency. The goal of this research was to interrogate and characterize the impact of obesity on the development of APL so as to provide a murine model for future

mechanistic studies of how obesity impacts the development and therapeutics of APL.

At the molecular level, APL is characterized by a reciprocal chromosomal translocation t(15;17), in which fusion of the gene for retinoic acid receptor α (*RARA*) on Ch17q21 with the gene for the transcription factor promyelocytic leukemia (*PML*) on Ch15q22 results in the gene fusion product *PML-RARA* (11-14). Knock-in mice bearing the human *PML-RARA* fusion gene were generated using homologous recombination to target the human fusion gene into the 5′ untranslated region of the murine cathepsin G (mCG) locus in C57BL/6J embryonic stem cells, which were subsequently implanted into pseudo-pregnant Swiss-Webster mice to generate the *PML-RARA* mouse (15). Offspring were crossed with C57BL/6J female mice, backcrossed, and intercrossed to generate heterozygous (B6.mCG$^{+/PR}$) and homozygous (B6.mCG$^{PR/PR}$) mice on the C57BL/6J background. Both heterozygous and homozygous mice bearing the *PML-RARA* fusion gene were shown to have high probability of developing an APL-like disorder at a median age of 10 months (6-19 months) (15).

We have previously shown that feeding a high-fat diet (HFD; 54% fat) versus a low-fat diet (LFD; 10.4% fat) to C57BL/6J mice bearing the *APC^{Min}* mutation leads to the development of obesity and promotes the development of intestinal neoplasia (16). Other tumors shown to be promoted by obesity in genetically predisposed mice have included pancreatic, hepatocellular, colorectal, prostate, breast, ovarian, endometrial, and esophageal cancers (3-10). Obesity in mice has also been shown to promote the growth of transplanted myeloma cells (17,18); however, to our knowledge, obesity has not been evaluated or shown to promote the development of hematologic malignancies in genetically predisposed animals. Using the B6.mCG$^{+/PR}$ mice fed an HFD and an LFD, we now report that obesity promotes and accelerates the development of APL in genetically predisposed mice.

Study Importance

What is already known?

- Acute promyelocytic leukemia (APL) in humans is increasingly being recognized as an obesity-associated malignancy.
- C57BL/6J mice containing the human promyelocytic leukemia (*PML*)-retinoic acid receptor α (*RARA*) fusion gene (C57BL/6J.mCG$^{+/PR}$) recapitulate the clinical components of APL.

What does this study add?

- APL in female mCG$^{+/PR}$ mice shows incomplete penetrance and delayed latency relative to male mice.
- Obesity accelerates the development of APL in both male and female mice and reduces sex differences in leukemia penetrance and latency.

How might these results change the direction of research?

- Results provide a robust and now carefully characterized mouse model to study sex differences in leukemia penetrance, as well as mechanisms of the impact of obesity on hematologic malignancies and response to therapy and/or weight loss.

METHODS

Animal studies

C57BL/6J (B6) mice were originally purchased from The Jackson Laboratory (Stock Number 000664), and C57BL/6J.mCG-*PML-RARA* (B6.mCG) mice were obtained from Timothy Ley, MD (Washington University School of Medicine, Saint Louis, St. Louis, Missouri). To establish specific pathogen free mCG mice, mCG preimplantation embryos were transferred into specific pathogen free pseudo-pregnant C57BL/6J recipient females and rederived in the Wolstein Animal Resource Center at Case Western Reserve University, Cleveland, Ohio. As noted earlier, these mice contain human *PML-RARA* complementary DNA inserted by homologous recombination in embryonic stem cells into the 5′ untranslated region of the mCG locus, thus targeting expression to early myeloid progenitor cells (15). All animals were housed in polysulfonate microisolator cages and maintained at 25°C on a 12-hour reverse light/dark cycle, as well as provided an autoclaved standard diet, Prolab Isopro RMH 3000 (P3000) from Lab Diet, and autoclaved water ad libitum. Colonies were propagated by placing single male B6.mCG$^{+/PR}$ mice with single female B6 mice, with breeding pairs maintained for approximately 1 year or until reproductive activity declined. Offspring were weaned and provided a standard chow diet (P3000) at 21 days of age.

At 30 days of age, mice were weighed, genotyped, as described later in this article, and randomly distributed between eight experimental conditions based on genotype, gender, and experimental diet, as follows: littermate control (B6.mCG$^{+/+}$) male mice fed an HFD, B6.mCG$^{+/+}$ male mice fed an LFD, B6.mCG$^{+/+}$ female mice fed an HFD, B6.mCG$^{+/+}$ female mice fed an LFD, B6.mCG$^{+/PR}$ mice fed an HFD, B6.mCG$^{+/PR}$ male mice fed an LFD, B6.mCG$^{+/PR}$ female mice fed an HFD, and B6.mCG$^{+/PR}$ female mice fed an LFD. Two to five mice were housed per cage while on the experimental diet and inspected by trained animal care technicians daily to assess general health status. Animal weights were measured and recorded weekly during light cycles. To screen for leukemia development, peripheral blood was collected via the retro-orbital sinus of anesthetized mice and analyzed through automated blood counting with a HemaVet 950 FS cell counter (Drew Scientific) at either 120, 180, 210, 280, or 360 days of age, with mice being bled ≤2 times throughout their life-span for a volume of ≤75 μL.

Mice were humanely killed when they became moribund or reached 500 days of age. Animals were euthanized by physical disruption of brain activity using cervical dislocation. At euthanasia, peripheral blood was obtained and aliquoted for automated complete blood analysis and plasma isolation. Plasma was snap frozen and stored at −80°C. Necropsy was performed, and spleens were collected, weighed, and fixed in 10% buffered formalin for histologic assessment. From the liver, left lobes were fixed in 10% buffered formalin, and caudate lobes were snap frozen for later analysis. Bone marrow was flushed from mouse femurs using phosphate-buffered saline (PBS) with 2% fetal bovine serum (FBS). Isolated bone marrow cells were aliquoted as follows: 0.5×10^5 cells were evenly deposited onto a microscope slide for histologic assessment via CytoSpin centrifuge (Thermo Fisher Scientific); aliquots of 1×10^5 cells were saved as dry pellets at −80°C; and the remaining sample was suspended in FBS with 10% dimethyl sulfoxide (DMSO), placed in a chilled Mr. Frosty controlled rate freezing container (Thermo Fisher Scientific), and transferred to a −80°C freezer for 24 hours before being stored in liquid nitrogen.

All mice were genotyped approximately 1 week after weaning using genomic DNA isolated from ear tissue via polymerase chain reaction (PCR). Primers for mCG-*PML-RARA* were forward (5′-GGCAGCAACTGACTAAGCAACGGTTCTGGA-3′) and reverse (5′-CAAGTGTATAGGACAGGACCTGATCTGAGG-3′ and 5′-CCGC TGCAGACTCTCGAAAA -3′). Littermate control ($mCG^{+/+}$) alleles displayed banding of 136 base pairs (bp), whereas mCG heterozygous ($mCG^{+/PR}$) and homozygous ($mCG^{PR/PR}$) animals displayed banding of 450 bp, with $mCG^{+/PR}$ animals showing bands at both 136 and 450 bp. Primer designs were obtained from Timothy Ley and ordered from Integrated DNA Technologies.

Experimental diets

Experimental diets, as previously described (19), were obtained from Research Diets Inc.: HFD (D12330: 58.0% kilocalories from fat [hydrogenated coconut oil], 25.5% kilocalories from carbohydrates [0 kcal sucrose, 700 kcal corn starch], 16.4% kcalories from protein); LFD (D12328: 10.5% kilocalories from fat [hydrogenated coconut oil], 73.1% kilocalories from carbohydrates [0 kcal sucrose, 3,340 kcal corn starch], 16.4% kilocalories from protein). Diets were formulated with AIN-76A Vitamin Mix (MP Biomedicals) and matched for caloric density and micronutrient content.

Immunohistochemistry and peripheral blood differential counts

Spleens were initially fixed in 10% buffered formalin for 24 hours before being embedded in paraffin and shipped to HistoWiz, Inc. (New York, New York). Samples were sectioned at 4 μm, after which histology was performed by HistoWiz using a standard operating procedure and fully automated workflow. Immunohistochemistry was performed on a Bond Rx autostainer (Leica Biosystems) with enzyme treatment (1:1000) using standard protocols. Antibodies used were rat monoclonal CD117 (c-kit), rabbit monoclonal CD11b, rabbit polyclonal CD20, rabbit monoclonal CD3, rabbit monoclonal CD34, and rabbit polyclonal Ki67. Bond Polymer Refine Detection (Leica Biosystems) was used according to the manufacturer's protocol. After staining, sections were dehydrated and film cover slipped using a TissueTek-Prisma and Coverslipper (Sakura Finetek USA). Whole-slide scanning (40×) was performed on an Aperio AT2 (Leica Biosystems).

Peripheral blood smears were prepared according to standard hematologic techniques and stained with Wright-Giemsa stain using a Sysmex XN-9000 Automated Hematology System (Sysmex Corporation). Microscopic white blood cell differentials were performed on peripheral blood smears by an experienced hematologist and reviewed by an experienced hematopathologist who were unaware of the experimental status of the animals of origin.

Statistics

GraphPad Prism (version 9; GraphPad Software Inc.) software was used for data visualization and statistical analyses. Unpaired Student *t* test and two-way ANOVA were used for comparison of differences between experimental groups. The Gehan-Breslow-Wilcoxon test and Fisher exact test were used to analyze leukemic incidence data. The specific statistical method employed for individual data sets is listed in the figure legends.

Study approval

All animal procedures were evaluated and approved prior to initiation by the Institutional Animal Care and Use Committee of the Case Western Reserve University School of Medicine.

RESULTS

Diet, sex, and genetic background determine body weight change and obesity

To determine the effects of diet-induced obesity (DIO) on leukemogenesis, we first examined the effects of diet, sex, and genetic background on body weight and obesity. Male and female littermate control mice ($B6.mCG^{+/+}$) and knock-in mice heterozygous for the *PML-RARA* fusion gene ($B6.mCG^{+/PR}$) were fed a calorically equivalent diet either high or low in hydrogenated coconut oil beginning at 30 days of age (Figure 1). Previously characterized weight responses to an HFD and an LFD in wild-type C57BL/6J (B6) mice were used to assess the weight response of each experimental cohort.

The weight gain of $B6.mCG^{+/+}$ mice recapitulated the responses to an HFD and an LFD observed in B6 animals (Figure 2A); therefore, these animals are representative models for observing the effects of DIO. Each experimental group showed significant variation in body

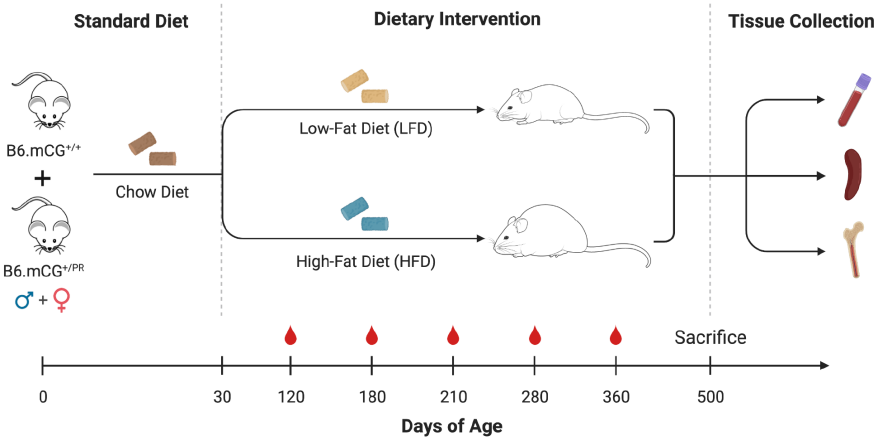

FIGURE 1 Diagram of study design for diet studies. Male and female B6.mCG$^{+/+}$ and B6.mCG$^{+/PR}$ mice were weaned and fed a standard chow diet from 21 days post partum until 30 days of age, at which point they were placed on either a high-fat or low-fat diet. Peripheral blood was collected via the retro-orbital sinus at 120, 180, 210, 280, 360, and 500 days of age. Spleens and bone marrow were collected via necropsy at 500 days of age or when animals became moribund. mCG, murine cathepsin G

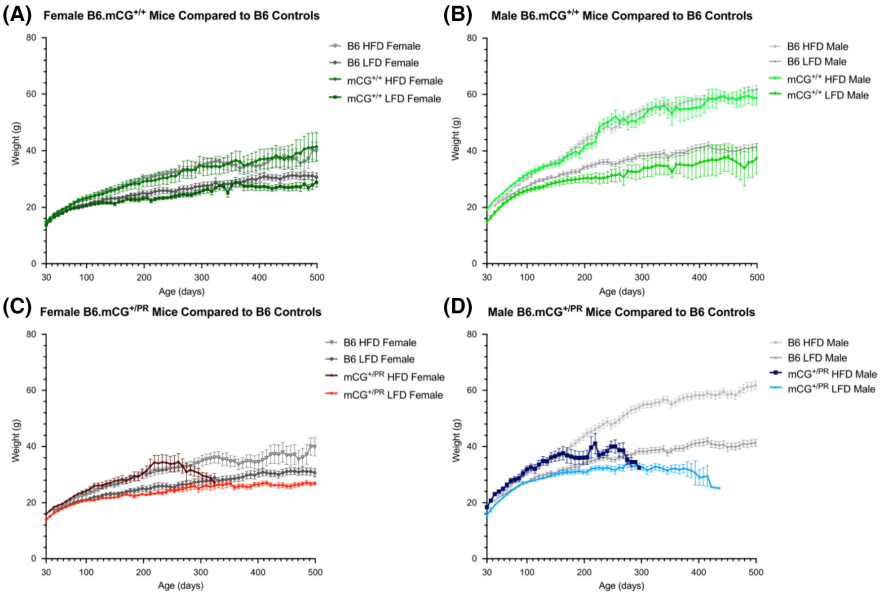

FIGURE 2 Diet, sex, and genetic background determine weight change and obesity. Body weight curves in grams for (A) female and (B) male B6.mCG$^{+/+}$ (green) mice and (C) female (red) and (D) male (blue) B6.mCG$^{+/PR}$ mice plotted alongside wild-type C57BL/6J (B6) control animals (gray) on HFD and LFD. Weights from individual mice were collected weekly and averaged, with error bars displaying the SEM. HFD, high-fat diet; LFD, low-fat diet; mCG, murine cathepsin G

weight based on diet and sex. HFD feeding resulted in significant increases in body weight in each group compared with LFD-fed animals, with female mice weighing 5 to 15 g less on average than male counterparts (Table 1). Although each HFD-fed group developed obesity by 100 days of age, animals displayed varying magnitudes of weight change contingent on genotype.

In contrast with littermate controls, whereas B6.mCG$^{+/PR}$ mice gained weight initially, these animals eventually exhibited weight loss that temporally coincided with the onset of disease (Figure 2B). Male B6.mCG$^{+/PR}$ mice fed an HFD diverged from their B6 counterparts at 170 days of age, aligning with the development of florid leukemia in these animals. LFD-fed male B6.mCG$^{+/PR}$ mice displayed a similar trend but began to deviate from the B6 weight curve at 220 days of age. Similarly, HFD-fed female B6.mCG$^{+/PR}$ mice diverged from their B6 counterparts at 265 days of age, whereas LFD-fed female B6.mCG$^{+/PR}$ mice deviated from the B6 weight curve at 360 days of age. These observations of weight loss in B6.mCG$^{+/PR}$ animals align closely with our recorded values of median leukemic incidence (Table 2), with declines in weight briefly preceding the manifestation of disease.

Obesity and obesogenic diet accelerate leukemia development in B6.mCG$^{+/PR}$ mice

To interrogate the association between DIO and leukemogenesis, we closely monitored the incidence of disease in each experimental

TABLE 1 Animal body weights by age, diet, sex, and genetic background

Cohort	100 days			250 days			500 days		
	LFD	HFD	*p* value	LFD	HFD	*p* value	LFD	HFD	*p* value
B6.mCG$^{+/+}$ male	25.98 (2.45) g $n = 10$	31.89 (2.28) g $n = 13$	***	31.26 (6.46) g $n = 10$	51.21 (6.98) g $n = 13$	***	32.74 (6.36) g $n = 4$	58.93 (6.67) g $n = 6$	***
B6.mCG$^{+/+}$ female	20.62 (1.47) g $n = 11$	23.45 (3.97) g $n = 17$	*	23.67 (2.21) g $n = 11$	31.08 (9.73) g $n = 17$	*	28.83 (4.60) g $n = 8$	41.35 (14.39) g $n = 8$	*
B6.mCG$^{+/PR}$ male	27.17 (1.49) g $n = 13$	31.90 (4.44) g $n = 13$	**	32.06 (3.26) g $n = 13$	39.97 (4.28) g $n = 5$	***	n/a	n/a	n/a
B6.mCG$^{+/PR}$ female	20.88 (1.47) g $n = 17$	24.12 (2.54) g $n = 12$	***	24.67 (3.16) g $n = 17$	33.83 (6.56) g $n = 6$	***	26.90 (1.30) g $n = 5$	n/a	n/a

Note: Mouse body weights for male and female, HFD- and LFD-fed, B6.mCG$^{+/+}$ and B6.mCG$^{+/PR}$ mice at 100, 250, and 500 days of age. Data shown as mean (SD).
Abbreviations: HFD, high-fat diet; LFD, low-fat diet; mCG, murine cathepsin G; n/a, not available because all mice had expired at that time.
*$p < 0.05$, as calculated by unpaired Student *t* test; **$p < 0.01$, as calculated by unpaired Student *t* test; ***$p < 0.001$, as calculated by unpaired Student *t* test.

animal using peripheral blood analysis. Prior characterization of the mCG-*PML-RARA* model identified a disease latency of 8 to 12 months and a penetrance of approximately 60% (15). Here, we demonstrate that latency and penetrance are impacted by sex and by dietary intervention (Figure 3; Table 2).

B6.mCG$^{+/PR}$ HFD-fed mice showed the earliest onset of leukemia (Figure 3). Male B6.mCG$^{+/PR}$ HFD-fed mice displayed an initial leukemia incidence at 144 days of age and a median incidence at 218 days of age. Although initial leukemia incidence in female B6.mCG$^{+/PR}$ HFD-fed mice preceded male counterparts by 37 days, females reached median leukemia incidence 54 days later than males (272 days). HFD also increased disease penetrance, with 100% of B6.mCG$^{+/PR}$ HFD-fed mice (both male and female) developing leukemia before 500 days of age. In contrast, LFD-fed B6.mCG$^{+/PR}$ animals exhibited longer latency periods and lower disease penetrance relative to their HFD-fed counterparts. Male B6.mCG$^{+/PR}$ mice fed an LFD began developing leukemia at 268 days of age, with a median leukemia incidence at 383 days and penetrance of 64.28%. LFD-fed female B6.mCG$^{+/PR}$ mice showed the greatest disease latency and lowest penetrance of all heterozygous animals, with earliest onset of leukemia occurring at 376 days of age, a median incidence of >500 days of age, and a penetrance of only 23.53% by the 500-day end-point of experimentation (Table 2). HFD accelerates the median incidence of leukemia in B6.mCG$^{+/PR}$ males by 157 days and in B6.mCG$^{+/PR}$ females by 228 days.

Examining APL penetrance and time to median penetrance in LFD-fed male compared with female B6.mCG$^{+/PR}$ mice showed a marked sex-dependent difference ($p = 0.0325$ and $p = 0.0011$, respectively). In both male and female B6.mCG$^{+/PR}$ mice, the HFD compared with the LFD clearly increased penetrance and shortened latency, demonstrating that an HFD and obesity accelerate the development of leukemia. In contrast with a sex difference in penetrance and latency of leukemia development among LFD-fed B6.mCG$^{+/PR}$ mice, there was no significant difference ($p = 0.1369$) in these parameters in HFD-fed mice, indicating that an HFD and obesity reduce the sex-dependent differences in APL onset in B6.mCG$^{+/PR}$ mice.

As displayed in Figure 3 and Table 2, leukemogenesis was not observed in any littermate control animal as of 500 days of age. This observation is in agreement with hundreds of B6 animals that have been studied on various obesogenic diets in the Berger laboratory, none of which has shown development of leukemia over the course of their life-span (unpublished).

Leukemic animals exhibit characteristic changes in peripheral blood

In humans, APL presents with a series of blood cell count abnormalities, including leukocytosis or leukopenia, with immaturity of myeloid cell series, progressive thrombocytopenia, and anemia. Through peripheral blood analyses, we have identified that B6.mCG$^{+/PR}$ mice emulate these phenotypes as part of disease development. In leukemic mice, we observed significantly higher concentrations of total leukocytes, granulocytes, and lymphocytes compared with

Obesity A Research Journal THE OBESITY SOCIETY –WILEY–

TABLE 2 Leukemia penetrance and incidence by cohort

Cohort	Cohort size	No. of leukemic animals	Cumulative penetrance	Median incidence
B6.mCG$^{+/+}$ HF female	17	0	0%	>500 days
B6.mCG$^{+/+}$ LF female	11	0	0%	>500 days
B6.mCG$^{+/+}$ HF male	13	0	0%	>500 days
B6.mCG$^{+/+}$ LF male	12	0	0%	>500 days
B6.mCG$^{+/PR}$ HF female	16	16	100%*	272 days
B6.mCG$^{+/PR}$ LF female	17	4	23.53%*,†	>500 days
B6.mCG$^{+/PR}$ HF male	13	13	100%*	218 days
B6.mCG$^{+/PR}$ LF male	14	9	64.28%*,†	383 days

Abbreviations: HF, high fat; LF, low fat; mCG, murine cathepsin G.

* $p < 0.001$ for evaluations performed between dietary counterparts.

† $p < 0.01$ for evaluations performed between sex counterparts as calculated by Gehan-Breslow-Wilcoxon tests.

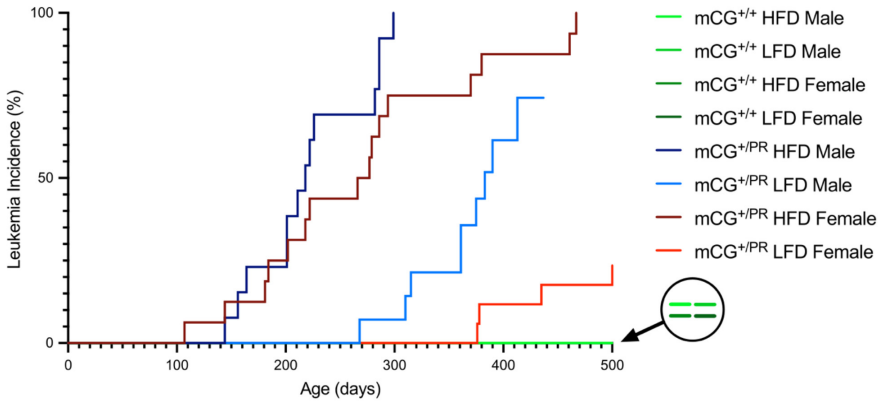

FIGURE 3 Obesogenic diet accelerates leukemia development in B6.mCG$^{+/PR}$ mice. Kaplan-Meier curves depicting cumulative incidence of leukemia in B6.mCG$^{+/+}$ HFD male ($n = 13$), LFD male ($n = 12$), HFD female ($n = 17$), and LFD female ($n = 11$) mice, as well as B6.mCG$^{+/PR}$ HFD male ($n = 13$), LFD male ($n = 14$), HFD female ($n = 16$), and LFD female ($n = 17$) mice. All B6.mCG$^{+/+}$ animals displayed 0% cumulative incidence of leukemia up to 500 days of age. HFD, high-fat diet; LFD, low-fat diet; mCG, murine cathepsin G

nonleukemic animals. Animals also manifest progressive thrombocytopenia during leukemia development, exhibiting significantly lower platelet concentrations in comparison with nonleukemic mice. In addition, leukemic animals become anemic, displaying significantly reduced hemoglobin and hematocrit relative to nonleukemic mice. It is also of note that no B6.mCG$^{+/+}$ mice were observed with peripheral blood counts indicative of a leukemic phenotype, reflecting their 0% cumulative leukemia incidence throughout the study. No obesity-dependent changes in peripheral blood counts were observed in nonleukemic mice. We did notice the presence of high leukocyte, granulocyte, and lymphocyte counts of leukemic animals, but a sensitivity analysis revealed that significance was still maintained even after the removal of these outliers.

Examination of peripheral blood of littermate control animals revealed normal lymphocytes and neutrophils (Figure 4A), as well as a complete absence of immature myeloid cells (myeloblasts, promyelocytes, myelocytes, and metamyelocytes; Figure 4C). Healthy B6.mCG$^{+/PR}$ mice initially showed this phenotype; however, with the development of leukemia, their peripheral blood revealed increased concentrations of immature myeloid precursors, with a particularly robust presence of promyelocytes (Figure 4D). These promyelocytes, which were also observed to be predominant in the spleen of leukemic animals (Figure 5C), were characterized by large cell size, round or oval nuclei, and an abundance of azurophilic granules in the cytoplasm (Figure 4B).

Leukemic animals display marked splenomegaly and histologic variations reminiscent of human APL

In addition to changes in the peripheral blood, clinical APL has been shown to present with progressive splenomegaly resulting from leukemic cell infiltration and extramedullary hematopoiesis. As previously noted (15), in both male and female leukemic B6.mCG$^{+/PR}$ mice, we observed marked splenomegaly (Figure 5A). There were virtually no differences between sexes in terms of the severity of splenomegaly. In addition, subtle variations were observed between dietary groups, with HFD-fed animals generally having heavier spleens at

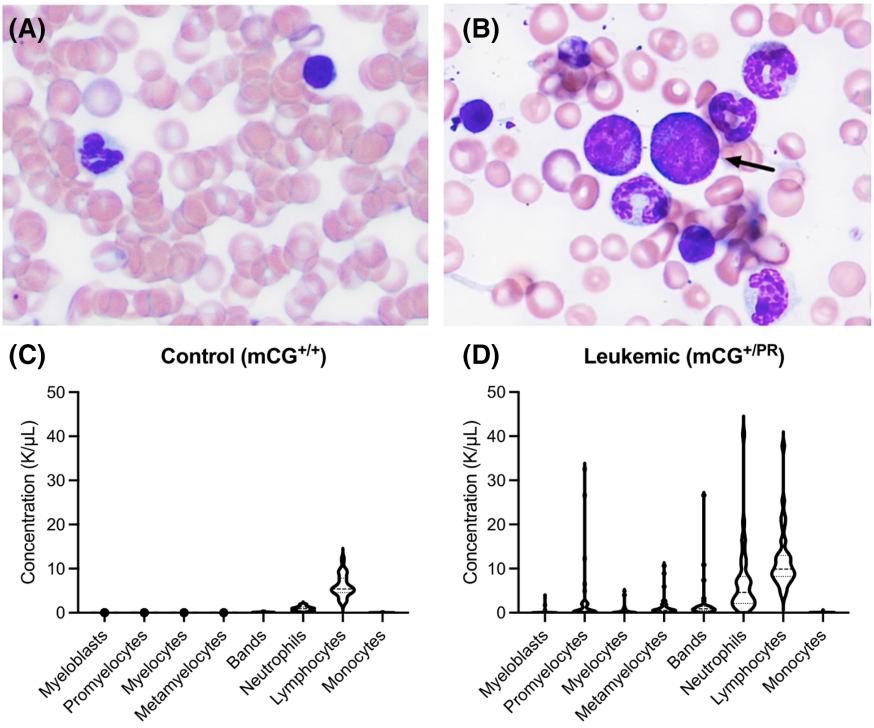

FIGURE 4 Peripheral blood from leukemic animals contains immature myeloid precursors. (A,B) Representative 100× images of peripheral blood collected from (A) a healthy B6.mCG$^{+/+}$ mouse and (B) a leukemic B6.mCG$^{+/PR}$ mouse (arrow indicates an immature myeloid series cell). Violin plots displaying concentrations of myeloblasts, promyelocytes, myelocytes, metamyelocytes, banded neutrophils (bands), segmented neutrophils, lymphocytes, and monocytes collected through manual differentials of peripheral blood smears from (C) healthy B6.mCG$^{+/+}$ ($n = 20$) and (D) leukemic B6.mCG$^{+/PR}$ ($n = 36$) mice (pooled low-fat diet and high-fat diet) isolated at death. Data displayed as median ± interquartile range. mCG, murine cathepsin G

death than their LFD-fed counterparts (Figure 5B). It is noteworthy that splenomegaly is associated with leukemia cell infiltration rather than as a direct result of an HFD alone, because B6.mCG$^{+/+}$ mice on an HFD showed no significant splenomegaly.

To characterize histologic and immunophenotypic variations in the spleens of normal and select leukemic animals, immunohistochemical staining was performed in addition to hematoxylin and eosin (H&E) staining on paraffin-embedded tissues. B6.mCG$^{+/+}$ mice displayed normal splenic architecture, consisting of white pulp containing lymphoid follicles with germinal centers and red pulp composed primarily of venous sinuses (Figure 5C). In contrast, the splenic architecture of leukemic animals was dramatically effaced (Figure 5C) by an excess of immature myeloid series cells, consisting mainly of myeloblasts and promyelocytes (Figure 5C), as well as increased megakaryocytes and hemophagocytic macrophages. Littermate control animals showed a normal distribution of CD3+ and CD20+ lymphocytes, as well as CD11b+ mature myeloid cells, with essentially no CD34+ cells and only focal Ki67 staining. In comparison, leukemic animals displayed numerous changes consistent with massive leukemic infiltration, including diffuse positivity for CD34, CD117, and Ki-67, with loss of mature cell markers (CD3+, CD20+, CD11b+; Figure 5D). Interestingly, although the predominant immunophenotype in human APL cases shows an absence of CD34 expression, the strong, diffuse CD34 staining present in our leukemic spleen samples reflects similar observations made by Westervelt et al. (15).

DISCUSSION

The growing prevalence of obesity has created a major public health concern owing to increased risk of multiple medical conditions, including hypertension, cardiovascular disease, diabetes mellitus, and specific forms of malignancy. Of the 13 cancers identified by the International Agency for Research on Cancer as having increased risk in the presence of excess body fatness (2), multiple myeloma remains the sole hematologic malignancy to have been declared an OAC. However, a growing body of literature has supported the notion that obesity acts as a risk factor for APL (1,20-24).

Here, we demonstrate that DIO accelerates the development and increases the penetrance of APL in genetically predisposed mice. In contrast with B6.mCG$^{+/+}$ littermate control animals, which were not observed to have developed disease and survived throughout the 500-day study period, B6.mCG$^{+/PR}$ mice displayed differential leukemic incidence and penetrance contingent on dietary intervention and sex. HFD-fed B6.mCG$^{+/PR}$ animals have shortened latency and increased penetrance of disease relative to LFD-fed counterparts. These data are supported by work performed by Westervelt et al. (15) and Mazzarella et al. (25), who have observed variations in disease-free survival from standard-chow diets and an HFD, respectively.

Our results clearly showed sex-dependent differences in the onset of APL in B6.mCG$^{+/PR}$ mice fed an LFD, with male mice

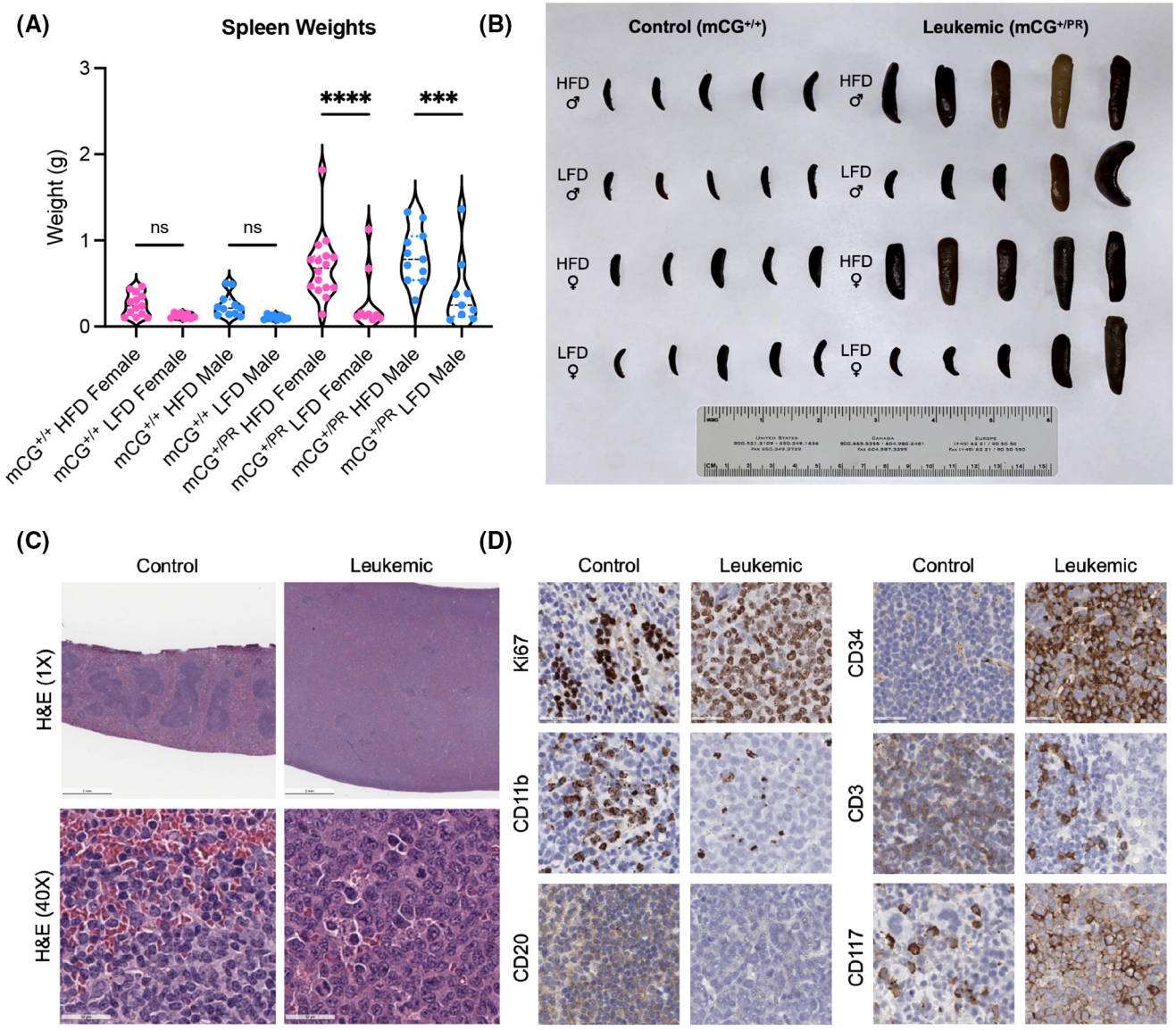

FIGURE 5 Leukemic animals develop marked splenomegaly and display variations in splenic architecture and immunophenotyping reflective of leukemic infiltration. (A) Violin plots displaying weight (grams) of spleens isolated at death from B6.mCG$^{+/+}$ HFD female (n = 13), LFD female (n = 8), HFD male (n = 11), and LFD male (n = 8) mice, as well as B6.mCG$^{+/PR}$ HFD female (n = 16), LFD female (n = 9), HFD male (n = 11), and LFD male (n = 9) mice. Data displayed as median ± interquartile range. (B) Representative image of the five heaviest spleens from each experimental cohort organized by genotype, gender, and diet. (C) Representative H&E-stained spleen sections from control (B6.mCG$^{+/+}$) and leukemic (B6.mCG$^{+/PR}$) animals; 1× (top row) and 40× (bottom row), with scale bars representing 2 mm and 50 μm, respectively. (D) Representative images depicting Ki67, CD11b, CD20, CD34, CD3, and CD117 immunohistochemical staining (brown) in serial sections of control (mCG$^{+/+}$) and leukemic (mCG$^{+/PR}$) murine spleen; 40×, scale bars (top row) represent 50 μm. ***$p < 0.001$; ****$p < 0.0001$. HFD, high-fat diet; LFD, low-fat diet; mCG, murine cathepsin G; ns, nonsignificant as determined by two-way ANOVA

showing 64.3% disease penetrance by 500 days and median latency at 383 days, compared with female mice, which showed only 23.5% penetrance and median latency greater than 500 days. HFD was shown to accelerate leukemia and reduce sex differences in penetrance and latency, such that high-fat feeding resulted in 100% penetrance in both male and female mice, with a median latency of 218 days in male mice and 272 days in female mice (p = 0.1369). The B6.mCG$^{+/PR}$ model indicates that an HFD and obesity accelerate the development of leukemia in genetically predisposed mice as opposed to inducing malignant transformation, because no leukemia was detected in HFD- or LFD-fed littermate control animals.

In addition to observing that DIO accelerates APL development *in vivo*, our data provide further evidence that genetic knock-in of the human *PML-RARA* fusion gene results in the manifestation of multiple clinical features characteristic of human APL. Not only did our study show the development of leukocytosis, progressive thrombocytopenia, anemia, and massive splenomegaly in leukemic mice, but histologic assessment also identified the presence of immature myeloid series cells, including promyelocytes, in the peripheral blood.

Immunohistochemical analyses revealed that leukemic animals displayed an immunophenotype similar to that of human APL, which is typically CD117+, CD11b−, and CD34− (26). While CD34 is most commonly absent in human APL, a small subset of cases do express this primitive hematopoietic marker (15,27,28), characteristic of less-differentiated APL myeloblasts.

We have previously shown in wild-type C57BL/6J mice fed with an HFD that male mice, compared with female mice, showed a more rapid increase in insulin resistance, circulating insulin, and retinol binding protein 4 (29). These observations, coupled with our current results, suggest the need for further studies of the impact of obesity on growth-regulating adipokines and hormones, as well as how these affect APL and sex differences in disease manifestations.

CONCLUSION

Our study demonstrates that obesity and an obesogenic diet not only accelerate APL development but also reduce sex differences in disease latency and penetrance. Nonetheless, it remains noteworthy that HFD-fed males began weight loss prior to HFD-fed females, indicating the persistence of some sex-dependent differences in disease effects among B6.mCG$^{+/PR}$ mice. These results raise the interesting question of the mechanism by which an HFD and obesity impact the development of APL as well as provide a robust model for interrogating the question. In addition, the potential for APL to be designated as an OAC should increase consideration of the use of targeted nutritional therapy, as recently demonstrated in mice and patients with obesity with acute lymphoblastic leukemia (30,31), and/or hormonal modification as adjuncts to the treatment of the malignancy.

ACKNOWLEDGMENTS

We thank Dr. Tim Ley, Washington University School of Medicine, St. Louis, Missouri, for his generous gift of C57BL/6J.mCG$^{+/PR}$ mice.

CONFLICT OF INTEREST

The authors declared no conflict of interest.

AUTHOR CONTRIBUTIONS

Concepts and experimental design were developed by John W. R. Kincaid and Nathan A. Berger. Conduct of research and data acquisition were performed by John W. R. Kincaid, Gretchen Weiss, Anne E. Hill-Baskin, Heidi M. Schmidt, Ovwoioise Omoijuanfo, Rose C. Beck, and Nathan A. Berger. Data analysis was performed by John W. R. Kincaid, Cheryl L. Thompson, and Nathan A. Berger. John W. R. Kincaid and Nathan A. Berger drafted the manuscript. All authors reviewed and approved the final manuscript.

ORCID

John W. R. Kincaid https://orcid.org/0000-0003-0660-9813
Nathan A. Berger https://orcid.org/0000-0001-7086-9885

REFERENCES

1. Mazzarella L, Botteri E, Matthews A, et al. Obesity is a risk factor for acute promyelocytic leukemia: evidence from population and cross-sectional studies and correlation with FLT3 mutations and polyunsaturated fatty acid metabolism. *Haematologica*. 2020;105:1559-1566.
2. Lauby-Secretan B, Scoccianti C, Loomis D, Grosse Y, Bianchini F, Straif K. Body fatness and cancer—viewpoint of the IARC working group. *N Engl J Med*. 2016;375:794-798.
3. Chung KM, Singh J, Lawres L, et al. Endocrine-exocrine signaling drives obesity-associated pancreatic ductal adenocarcinoma. *Cell*. 2020;181:832-847.e18.
4. Thompson KJ, Swan RZ, Walling TL, Iannitti DA, McKillop IH, Sindram D. Obesity, but not ethanol, promotes tumor incidence and progression in a mouse model of hepatocellular carcinoma in vivo. *Surg Endosc*. 2013;27:2782-2791.
5. Newmark HL, Yang K, Lipkin M, et al. A Western-style diet induces benign and malignant neoplasms in the colon of normal C57Bl/6 mice. *Carcinogenesis*. 2001;22:1871-1875.
6. Xue L, Yang K, Newmark H, Lipkin M. Induced hyperproliferation in epithelial cells of mouse prostate by a Western-style diet. *Carcinogenesis*. 1997;18:995-999.
7. Cleary MP. Impact of obesity on development and progression of mammary tumors in preclinical models of breast cancer. *J Mammary Gland Biol Neoplasia*. 2013;18:333-343.
8. Liu Y, Metzinger MN, Lewellen KA, et al. Obesity contributes to ovarian cancer metastatic success through increased lipogenesis, enhanced vascularity, and decreased infiltration of M1 macrophages. *Cancer Res*. 2015;75:5046-5057.
9. Yu W, Cline M, Maxwell LG, et al. Dietary vitamin D exposure prevents obesity-induced increase in endometrial cancer in Pten+/- mice. *Cancer Prev Res (Phila)*. 2010;3:1246-1258.
10. Quante M, Bhagat G, Abrams JA, et al. Bile acid and inflammation activate gastric cardia stem cells in a mouse model of Barrett-like metaplasia. *Cancer Cell*. 2012;21:36-51.
11. de Thé H, Chomienne C, Lanotte M, Degos L, Dejean A. The t(15;17) translocation of acute promyelocytic leukaemia fuses the retinoic acid receptor α gene to a novel transcribed locus. *Nature*. 1990;347:558-561.
12. Longo L, Pandolfi PP, Biondi A, et al. Rearrangements and aberrant expression of the retinoic acid receptor alpha gene in acute promyelocytic leukemias. *J Exp Med*. 1990;172:1571-1575.
13. Lemons RS, Eilender D, Waldmann RA, et al. Cloning and characterization of the t(15;17) translocation breakpoint region in acute promyelocytic leukemia. *Genes Chromosomes Cancer*. 1990;2:79-87.
14. Alcalay M, Zangrilli D, Pandolfi PP, et al. Translocation breakpoint of acute promyelocytic leukemia lies within the retinoic acid receptor alpha locus. *Proc Natl Acad Sci USA*. 1991;88:1977-1981.
15. Westervelt P, Lane AA, Pollock JL, et al. High-penetrance mouse model of acute promyelocytic leukemia with very low levels of PML-RARα expression. *Blood*. 2003;102:1857-1865.
16. Doerner SK, Reis ES, Leung ES, et al. High-fat diet-induced complement activation mediates intestinal inflammation and neoplasia, independent of obesity. *Mol Cancer Res*. 2016;14:953-965.
17. Lwin ST, Olechnowicz SWZ, Fowler JA, Edwards CM. Diet-induced obesity promotes a myeloma-like condition in vivo. *Leukemia*. 2015;29:507-510.
18. Campbell HF, Marinac CR, Masarwi M, Birmann B, Reagan M. Investigation of the relationship between obesity, weight cycling, and tumor progression in a myeloma xenograft model [abstract]. *Clin Lymphoma Myeloma Leuk*. 2019;19(suppl):e88.
19. Surwit RS, Feinglos MN, Rodin J, et al. Differential effects of fat and sucrose on the development of obesity and diabetes in C57BL/6J and A/J mice. *Metabolism*. 1995;44:645-651.

20. Poynter JN, Richardson M, Blair CK, et al. Obesity over the life course and risk of acute myeloid leukemia and myelodysplastic syndromes. *Cancer Epidemiol*. 2016;40:134-140.
21. Li S, Chen LI, Jin W, et al. Influence of body mass index on incidence and prognosis of acute myeloid leukemia and acute promyelocytic leukemia: a meta-analysis. *Sci Rep*. 2017;7:17998. doi:10.1038/s41598-017-18278-x
22. Kashanian SM, Li AY, Mustafa Ali M, et al. Increased body mass index is a risk factor for acute promyelocytic leukemia. *EJHaem*. 2021;2:33-39.
23. Breccia M, Mazzarella L, Bagnardi V, et al. Increased BMI correlates with higher risk of disease relapse and differentiation syndrome in patients with acute promyelocytic leukemia treated with the AIDA protocols. *Blood*. 2012;119:49-54.
24. Tedesco J, Qualtieri J, Head D, Savani BN, Reddy N. High prevalence of obesity in acute promyelocytic leukemia (APL): implications for differentiating agents in APL and metabolic syndrome. *Ther Adv Hematol*. 2011;2:141-145.
25. Mazzarella L, Durfort T, Pelicci PG. Modelling the influence of diet on APL identifies insulin-growth factor 1 as a central mediator and provides a mechanistic rationale for therapeutic weight loss [abstract]. *Blood*. 2013;122:833.
26. Horna P, Zhang L, Sotomayor EM, Lancet JE, Moscinski LC. Diagnostic immunophenotype of acute promyelocytic leukemia before and early during therapy with all-trans retinoic acid. *Am J Clin Pathol*. 2014;142:546-552.
27. Foley R, Soamboonsrup P, Carter RF, et al. CD34-positive acute promyelocytic leukemia is associated with leukocytosis, microgranular/hypogranular morphology, expression of CD2 and bcr3 isoform. *Am J Hematol*. 2001;67:34-41.
28. Gorczyca W. Acute promyelocytic leukemia: four distinct patterns by flow cytometry immunophenotyping. *Pol J Pathol*. 2012;63:8-17.
29. Bakshi S, Schmidt HM, Baskin AE, et al. Sexual dimorphism in developmental and diet-dependent circulating retinol binding protein 4. *Obes Sci Pract*. 2018;4:526-534.
30. Tucci J, Alhushki W, Chen T, Sheng X, Kim Y-M, Mittelman SD. Switch to low-fat diet improves outcome of acute lymphoblastic leukemia in obese mice. *Cancer Metab*. 2018;6:15. doi:10.1186/s40170-018-0189-0
31. Orgel E, Framson C, Buxton R, et al. Caloric and nutrient restriction to augment chemotherapy efficacy for acute lymphoblastic leukemia: the IDEAL trial. *Blood Adv*. 2021;5:1853-1861.

How to cite this article: Kincaid JWR, Weiss G, Hill-Baskin AE, et al. Obesity accelerates acute promyelocytic leukemia in mice and reduces sex differences in latency and penetrance. *Obesity (Silver Spring)*. 2022;30:1420–1429. doi:10.1002/oby.23435